 FDMP, vol.3, no.3, pp.189-202, 2007

Oxygen Transport in Tissue Engineering Systems: Cartilage and Myocardium

B. Obradovic[1], M. Radisic[2], G. Vunjak-Novakovic[3]

Abstract: Efficient transport of oxygen is one of the main requirements in tissue engineering systems in order to avoid cell death in the inner tissue regions and support uniform tissue regeneration. In this paper, we review approaches to design of tissue engineering systems with adequate oxygen delivery for cultivation of cartilage and myocardium, two distinctly different tissue types with respect to the tissue structure and oxygen requirements. Mathematical modeling was used to support experimental results and predict oxygen transport within the cultivated tissues and correlate it to the cell response and tissue properties.

Keyword: tissue engineering, oxygen transport, cartilage, myocardium, mathematical modeling

1 Introduction

Tissue engineering is one of the new strategies aimed at addressing the clinical problem of tissue failure by providing functional, biological substitutes of compromised native tissues. Ideally, lost or damaged tissue could be replaced by an engineered graft that can re-establish appropriate structure, composition, cell signaling, and function of the native tissue. In addition, functional constructs can also serve as physiologically relevant models for *in vitro* studies of tissue development and help distinguishing the effects of specific environmental signals from the complex milieu of factors present *in vivo.*

One approach to tissue engineering is *in vitro* cultivation of functional tissue equivalents by mimicking the native cell environment and recapitulating processes during normal *in vivo* tissue development. This approach is generally based on reparative cells, a structural template, and bioreactor cultivation that provides facilitated transport of nutrients and metabolites, as well as molecular and mechanical regulatory factors. These studies are aimed at establishing fundamental correlations between *in vitro* cultivation conditions, cell response, and resulting structural and functional properties of the engineered tissue. Mathematical modeling is an indispensable tool in the analysis of such complex systems, generally applied to determine at least one of the following: (*i*) define *in vitro* cultivation conditions, (*ii*) characterize engineered tissues, and (*iii*) correlate cultivating conditions with the cell response and tissue properties.

In this paper, we review mass transfer conditions in tissue engineering bioreactors as well as mathematical modeling approaches used to describe and correlate mass transfer rates to the tissue properties. In particular, transport of oxygen is considered since it is limiting even in conventional 2D cultures (Randers-Eichorn et al., 1996) and becomes critically inadequate in 3D tissue structures (Martin et al., 2004; Muschler et al., 2004). Efficient oxygen delivery to the cells is one of the main requirements in tissue engineering systems in order to achieve tissue uniformity and avoid widespread cell-death in the inner regions of scaffolds.

Integrated design of tissue engineering bioreactors and cell support configuration should provide mass transfer rates suited to particular tissue organization and cell metabolism. In this paper, we review approaches to design of tissue engineering systems with appropriate transport of oxygen for

[1] Faculty of Technology and Metallurgy, Belgrade University, Belgrade, Serbia
[2] University of Toronto, Toronto, Ontario, Canada
[3] Columbia University, New York, NY, U.S.A.

engineering of cartilage and myocardium, two tissue types with distinctly different structures and requirements for oxygen supply.

2 Cartilage tissue engineering

Skeletally mature articular cartilage is an avascular tissue composed of relatively low number of cells (chondrocytes) embedded in abundant extracellular matrix (ECM), consisting of a fibrous network of collagen type II and glycosaminoglycan (GAG)-rich proteoglycans (Buckwalter and Mankin, 1997). It is supplied by oxygen and nutrients from the synovial fluid by a combination of molecular diffusion through the tissue and "physiologic pump" transport, associated with joint loading and cartilage deformation during normal activities (O'Hara et al., 1990). Concentrations of dissolved oxygen range from 45 to 57 mmHg at the cartilage surface to less than 7.6 mmHg in the deep zone (Brighton and Heppenstall, 1971; Urban, 1994). Chondrocytes are therefore well adapted to hypoxic conditions and provide normal turnover of the ECM in healthy tissue. However, adult cartilage under physiologic conditions has practically no capacity for self-repair after an injury. In contrast, immature cartilage is vascularized and efficiently supplied with oxygen and nutrients and exhibits high biosynthetic activity.

Rotating bioreactors were shown to provide oxygen transport sufficient to meet relatively low oxygen requirements of cartilage and promote chondrogenesis (Obradovic et al., 2000). In this bioreactor type, the level of oxygen in culture medium is controlled via gas exchange with incubator air and oxygen is transferred to the tissue surfaces via convection while the internal transport of oxygen throughout the tissue is governed by diffusion.

2.1 Bioreactor culture system

Cell-polymer constructs were prepared by seeding chondrocytes isolated from full thickness cartilage into 5 mm diameter by 2 mm thick scaffolds made of fibrous polyglycolic acid (PGA) (Vunjak-Novakovic et al., 1998). After 3 days of seeding, cell-polymer constructs were transferred into the annular space of bioreactors (typically 11 constructs per bioreactor), configured as two concentric cylinders (Fig. 1a). Each bioreactor was rotating around its central horizontal axis such that the constructs were suspended in the rotating flow of the culture medium. The vessel rotation rate was adjusted to maintain each construct settling at a stationary point within the vessel. The flow conditions were dynamic and laminar, with tissue constructs settling in a tumble-slide regime associated with fluctuations in fluid pressure, velocity, and shear (Freed and Vunjak-Novakovic, 1995). The incubator gas was continuously pumped through the porous, inner cylinder covered by a silicone membrane providing continuous gas exchange and maintaining oxygen level in the culture medium at about 80 mmHg (Obradovic at al, 1999). Exceptionally, in studies of the oxygen effects on *in vitro* chondrogenesis, gas exchange was eliminated by using a solid inner cylinder in the otherwise identical bioreactor, which resulted in the oxygen level of $\sim$ 40 mmHg in the culture medium (Obradovic 1999). Mass transport between the culture medium and tissue constructs was enhanced by dynamic laminar convection, whereas the transport within the tissue remained governed by molecular diffusion.

2.2 In vitro tissue chondrogenesis

Under normal oxygen tensions in the culture medium in rotating bioreactors ($\sim$ 80 mmHg), engineered constructs progressively deposited ECM components over the cultivation time (Fig 1b). Chondrogenesis started at the construct periphery and over time, progressed both inward towards the construct center and outward from its surface, resulting in significant increase in the construct size and weight. By 6 weeks of culture, self-regulated cell proliferation and deposition of cartilaginous matrix yielded constructs that had physiological cell density and spatially uniform distributions of matrix components comprising 75% as much GAG, and 40% as much total collagen (hydroxyproline) per unit wet weight as normal cartilage (Vunjak-Novakovic et al., 1999).

In contrast to the cultures at normal oxygen tensions, cultivation at relatively low oxygen tensions under otherwise identical conditions in ro-

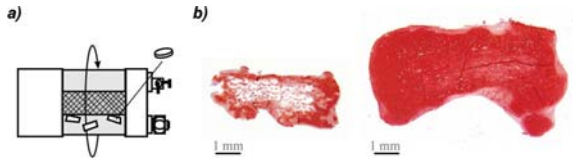

Figure 1: Tissue chondrogenesis in rotating bioreactors at normal oxygen tensions ($\sim$ 80 mmHg). a) Rotating bioreactor consisted of two concentric cylinders with tissue constructs suspended in the annular space. Bioreactor rotation provided suspension of the constructs in the culture medium settling at a stationary point. Gas exchange was provided by pumping the incubator gas through the porous, inner cylinder covered by a silicone membrane. b) Histological cross-sections of cell-polymer constructs cultivated in rotating bioreactors for 10 days (left) and 6 weeks (right); safranin O stain.

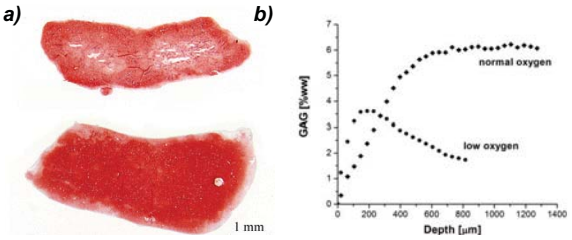

Figure 2: Effect of oxygen tension on tissue chondrogenesis in rotating bioreactors. a) Histological cross-sections of cell-polymer constructs cultivated for 5 weeks at low ($\sim$ 40 mmHg) (upper panel) and normal ($\sim$ 80 mmHg) oxygen tensions (bottom panel); safranin O stain. b) GAG distribution within the tissue constructs cultivated for 5 weeks at low ($\sim$ 40 mmHg) and normal ($\sim$ 80 mmHg) oxygen tensions, determined by image analysis of histological cross-sections as a function of the tissue depth starting from the construct surface. Adapted with modifications from Obradovic et al., 1999.

tating bioreactors, resulted in significantly lower and non-uniform ECM deposition and yielded significantly smaller engineered constructs. After 5 weeks of cultivation at low (42.7 $\pm$ 4.5 mmHg) and normal (86.5 $\pm$ 7.3 mmHg) oxygen tensions, engineered constructs had 101 $\pm$ 8 and 139 $\pm$ 12 mg wet weight, 3.07 $\pm$ 0.28 and 4.18 $\pm$ 0.22 %ww GAG, and 0.77 $\pm$ 0.03 and 2.76 $\pm$ 0.03 %ww collagen, respectively (Obradovic et al., 1999). ECM components in constructs cultivated at low oxygen tensions were deposited mostly at the construct periphery in contrast to morphological appearances of constructs cultivated at normal oxygen tensions, which had rather uniform distributions of ECM components (Fig. 2).

Similar effect of oxygen was found in cultures of cartilage explants, in which a decrease in medium oxygen tension from $\sim$ 80 mmHg to $\sim$ 40 mmHg resulted in a shift from aerobic to anaerobic cell metabolism and eventually suppressed the tissue growth (Obradovic et al., 1997).

2.3 Mathematical model

In order to interpret experimental findings of tissue growth and ECM deposition and to quantify the effects of oxygen, a mathematical model was formulated, which yielded concentrations of glycosaminoglycan (GAG) as a function of time and position within constructs cultivated in rotating bioreactors (Obradovic et al., 2000). Production of GAG was taken as a marker of chondrogenesis based on previous findings that GAG deposition in engineered constructs coincided with deposition of collagen type II, the other major component of cartilage tissue matrix (Freed et al., 1998). In order to validate the model, a high-resolution (40 μm) image analysis method was applied to measure the local GAG concentrations in histological tissue sections (Martin et al., 1999).

GAG concentration profiles within tissue constructs can be analyzed as a function of GAG synthesis by the cells, diffusion of newly synthesized and not yet incorporated and immobilized GAG and the resulting accumulation within the tissue matrix. The governing equation for GAG distribution within a disc-shaped tissue construct over the cultivation time, t, is:

$$\frac{\partial C_G}{\partial t} = D_G \left(\frac{\partial^2 C_G}{\partial r^2} + \frac{1}{r}\frac{\partial C_G}{\partial r} + \frac{\partial^2 C_G}{\partial z^2} \right) + Q_G \quad (1)$$

where r and z are cylindrical coordinates (GAG

concentration is independent of θ due to symmetry), C_G is the GAG concentration, D_G is the coefficient of GAG diffusion within the tissue, and Q_G is the rate of GAG synthesis. In healthy cartilage *in vivo*, GAG concentration within the tissue is maintained at a constant level by a balance between GAG synthesis and catabolism (Hascall et al., 1999). Accordingly, GAG synthesis rate was formulated as product inhibited with C_l as the maximum GAG concentration, corresponding to that found *in vivo*. In addition, the central hypothesis of the model was that the rate of GAG synthesis depends on the local oxygen concentration (C_{O2}) according to the first order kinetics. The GAG synthesis rate can be then expressed as:

$$Q_G = \rho \cdot k \cdot \left(1 - \frac{C_G}{C_l}\right) \cdot C_{O_2} \tag{2}$$

where ρ is the cell density, and k is the apparent synthesis rate constant, which incorporated the effects of all other parameters affecting GAG synthesis rate.

Oxygen concentration within the tissue was assumed to be governed by oxygen transport from the culture medium to the cells and cellular consumption modeled as Michaelis-Menten kinetics, that is:

$$\frac{\partial C_{O_2}}{\partial t} = D_{O_2}\left(\frac{\partial^2 C_{O_2}}{\partial r^2} + \frac{1}{r}\frac{\partial C_{O_2}}{\partial r} + \frac{\partial^2 C_{O_2}}{\partial z^2}\right) - \rho \cdot \frac{Q_m C_{O_2}}{C_m + C_{O_2}} \tag{3}$$

where D_{O2} is the oxygen diffusion coefficient in constructs, Q_m is the maximum rate of oxygen consumption, and C_m is the C_{O2} at the half-maximum consumption rate.

Negligible mass transfer resistances from the culture medium to the tissue surfaces were assumed, yielding initial and boundary conditions listed in the Table 1.

In order to incorporate appreciable tissue growth over time (Fig. 1b), construct diameter (d) and thickness (h) were forced to vary according to experimental observations. The resulting changes in cell density (ρ) were experimentally determined by image analysis of histological cross-sections of samples taken at different time points and interpolated as a function of time (Obradovic et al., 2000). The final cell density was about 1.2×10^8 cell/ml, which is close to the physiologic cell density. The limiting GAG concentration, C_l, was determined by image analysis of histological cross-sections of constructs cultured for 5 to 6 weeks in rotating bioreactors and the average value of 5.5%ww was applied in the model. GAG diffusion coefficient, D_G, was estimated from measured rates of GAG release into the culture medium and the corresponding concentration gradients at the construct surfaces, using the following transport equation:

$$V_{med}\frac{dC_{Gmed}}{dt} = D_G S \left.\frac{\partial C_G}{\partial \delta}\right|_{\delta=0} \tag{4}$$

where V_{med} is the volume of medium, C_{Gmed} is the measured GAG concentration in medium, S is the construct surface area, and δ is the construct depth starting from the construct surface ($\delta = 0$). The apparent D_G was estimated as 7×10^{-11} cm^2/s (Obradovic et al., 2000). The maximum rate of oxygen consumption, Q_m, was experimentally determined in the construct cultures

Table 1: Initial and boundary conditions for a construct of a diameter d, and thickness h: GAG and O_2 concentrations within the tissue were assumed initially to be equal to those measured in the culture medium; GAG and O_2 concentrations at the tissue surfaces were assumed to be equal to those measured in the culture medium at all times; symmetry conditions were applied along construct axes.

Initial conditions	$t = 0$	$0 \le r < d/2$; $0 \le z < h/2$	$C_G = 0^*$ $C_{O_2} = C^o_{O_2}{}^*$
Boundary conditions	$t \ge 0$	$r = d/2$; $0 \le z \le h/2$ $z = h/2$; $0 \le r \le d/2$	$C_G = 0$ $C_{O_2} = C^o_{O_2}$
		$r = 0$; $0 \le z \le h/2$	$\frac{\partial C_G}{\partial r} = 0$
		$z = 0$; $0 \le r \le d/2$	$\frac{\partial C_G}{\partial z} = 0$

* GAG concentration measured in the culture medium was negligible as compared to that determined in constructs; $C^o_{O_2}$ is the O_2 concentration measured in the culture medium (0.125 mM).

as 1.86×10^{-18} mole/cell.s. Michaelis-Menten constant, C_m, and oxygen diffusion coefficient, D_{O_2}, were set to 6.0 μM and 1.5×10^{-5} cm^2/s, as reported in literature (Haselgrove et al., 1993). All other parameters affecting GAG synthesis rate were lumped into the synthesis rate kinetic constant, k. However, k was observed to increase with time so that the change of k with time, t, was incorporated into the model based on the experimental evidence (Freed et al., 1998), as:

$$k = k_o[1 + A(t - t_o)]; \quad t \geq t_o = 12 \text{ days} \qquad (5)$$

where k_o is the apparent kinetic rate of GAG synthesis in the initial culture period t_o, and $A = 0.11$ day^{-1} is the experimentally determined parameter. The increase in k was not observed at low oxygen tensions ($A = 0$). The governing equations (eq. (1) with incorporated eqs (2) and (5) for GAG and eq. (3) for O_2) were solved numerically. The only adjustable parameter k_o was determined by a least-squares fit of the model to the experimentally determined GAG concentration profile in constructs cultured for the initial 10 days.

The model predicted a gradual decrease of oxygen concentration from the construct surface towards its center, as a result of oxygen consumption by the cells. Due to the higher total number of cells and larger diffusion distances, the decrease in oxygen concentration was markedly higher in 6-week as compared to 10-day constructs (Fig. 3a). Model predictions for concentration profiles of GAG were in excellent qualitative and quantitative agreement with those measured via image processing of tissue samples (average SD = $\pm$ 0.2 % wet weight GAG; Fig. 3b). In addition, the model was also validated by satisfactory predictions of GAG concentration profiles in constructs cultivated under low oxygen tension assuming the constant k_o (Obradovic et al., 2000).

The consistency of model predictions with experimental data implies that even though the model only grossly approximated the processes during *in vitro* chondrogenesis, it incorporated the main rate-controlling steps and the simplifications did not distort actual behavior. The modeling could be further extended to incorporate predictions of

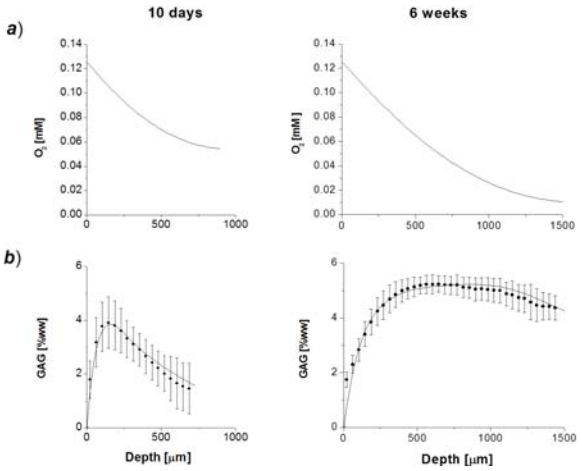

Figure 3: Mathematical modeling of *in vitro* chondrogenesis in rotating bioreactors at normal oxygen tensions. a) Model predictions of oxygen distribution within the cell-polymer constructs at 10 days and 6 weeks. b) Model predictions (lines) and experimental data (symbols) of GAG concentration profiles within the constructs at 10 days and 6 weeks; (based on data reported in Obradovic et al., 2000).

the tissue growth that is assumed to be stimulated by the fluid shear stress (Lappa, 2003) and formulated as a moving boundary problem (e.g. Lappa, 2003, 2005; Hogea et al., 2005, 2006). However, the present model revealed the importance of oxygen concentration for GAG synthesis in engineered cartilage, especially in the beginning of cultivation (about 10 days). As chondrogenesis progressed beyond the initial period of cultivation, GAG synthesis rate constant increased only if sufficiently high oxygen concentration in the culture medium was provided. At these conditions, corresponding to the normal cultivating conditions in rotating bioreactors, diffusion of oxygen within the cell-polymer constructs was sufficient to induce and support uniform GAG deposition.

3 Cardiac tissue engineering

The myocardium is a highly differentiated tissue that couples electrical and mechanical sig-

nals to provide blood flow throughout the organism. It is composed of cardiac myocytes, endothelial cells, and fibroblasts with a dense supporting vasculature and collagen-based extracellular matrix. Cardiomyocytes comprise only 20-40% of the cells in the heart but they occupy 80-90% of the heart volume. The high metabolic activity is supported by the high density of mitochondria in the cells (MacKenna et al., 1994; Brilla et al., 1995), and vast amounts of oxygen supplied by convective blood flow through the capillary network and by diffusion into the tissue space surrounding each capillary. Under physiologic conditions, oxygen dissolved in blood plasma accounts for only $\sim$1.5% of total oxygen content of the blood (Fournier, 1998) while the majority of oxygen carrying capacity of the blood comes from hemoglobin, a natural oxygen carrier.

In conventional cardiac tissue engineering approaches, medium flow provided convective transport of oxygen to the construct surfaces and molecular diffusion provided oxygen through the construct interior, resulting in tissues with $\sim$100 μm thick outer layer of viable cells and hypoxic, acellular or necrotic core (Bursac et al., 1999).

In order to enhance oxygen supply to the cells within engineered constructs, we adopted a biomimetic approach, where oxygen is supplied to the cells by mechanisms similar to those in the native heart. Highly porous, channeled scaffolds, culture medium supplemented with oxygen carriers, and perfusion bioreactors were utilized to provide convective transport of oxygen through the tissue constructs mimicking *in vivo* mechanisms of oxygen delivery to the cells (Radisic et al., 2006a, Radisic et al., 2006b).

3.1 Effect of oxygen on cardiac cell viability

In order to correlate local oxygen concentration with spatial distribution of viable cardiomyocytes, cardiac tissue constructs were prepared by seeding neonatal rat ventricular myocytes into collagen sponges (6 mm diameter discs, 1.5 mm thick) at an initial cell density within physiologic range (1.5×10^8 cells/cm^3) (Radisic et al., 2003). Constructs were cultivated for 16 days in static dishes, and at the end of cultivation, oxygen profiles were measured under static conditions. Oxygen tension was measured from the top to the bottom surface of the construct at four equally spaced locations using a modified Clark electrode, with a 4 μm tip (Malda et al., 2004). Distribution of cell viability was obtained by image analysis of histological cross sections of constructs stained with Reduced Biohazard Cell ViabilityKit (Molecular Probes).

Oxygen concentrations measured in the constructs under static conditions steadily decreased over the tissue depth resulting in $\sim$20 μM at the bottom tissue surface (Fig. 4a). Similarly, total cell density and the fraction of viable cells decreased over the tissue depth resulting in an exponential decay of the density of live cells (Fig. 4b) (Radisic et al., 2006c). Furthermore, live cell density could be correlated to the local oxygen concentration as:

$$\rho = \alpha e^{-\beta C_{O_2}} \tag{6}$$

where ρ is the live cell density (10^8 cell/cm^3), α and β are parameters estimated as $\alpha = 4 \times 10^4$ cell/cm^3, $\beta = 0.0518 \mu\text{M}^{-1}$, and C_{O2} is the local oxygen concentration (μM). High cell viability ($\geq$60%) was maintained at concentrations of oxygen above 120 μM. The decrease in oxygen concentration below 70 μM (at $\sim$1 mm beneath the construct surface) led to the decrease in viability to below 20% (Radisic et al., 2006c).

Results of this study clearly indicated the need for efficient delivery of oxygen in cardiac constructs such that oxygen concentration is maintained above $\sim$ 100 μM at all points within the engineered tissue.

3.2 Biomimetic bioreactor culture system

To mimic the capillary network, rat cardiomyocytes alone or in co-culture with fibroblasts isolated from 1 – 2 day old neonatal rats were seeded on a highly porous elastomer (Wang et al., 2002) with a parallel array of channels (Radisic et al, 2006a). Gel–cell inoculated constructs (5-6 mm diameter x 2 mm thick discs) were fitted into 1.5-ml polycarbonate perfusion cartridges (1 construct per cartridge) between two O rings (5 mm ID, 10 mm OD) and stainless steel screens, in order to provide medium flow directly through the

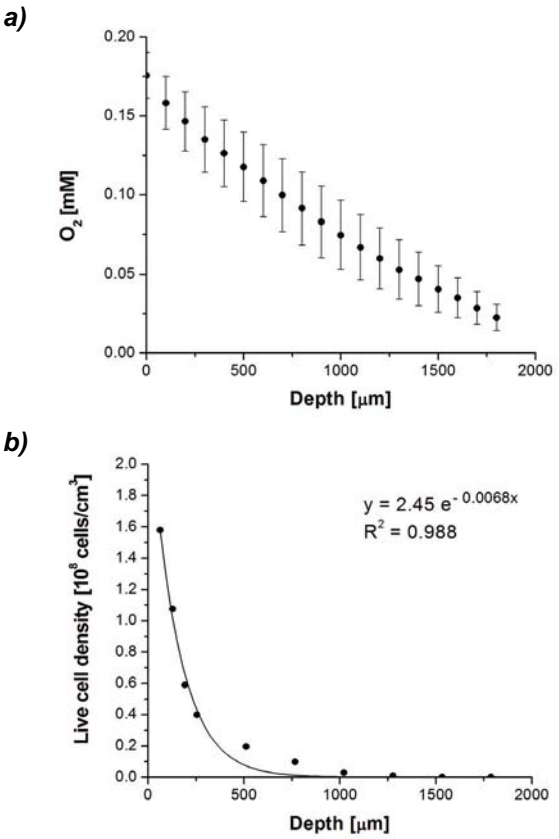

Figure 4: Effects of oxygen concentration on cell viability. a) Oxygen concentration along cross sections of statically cultured cardiac constructs for 16 days (n=4 constructs). The average construct thickness is 1.84±0.08 mm. b) Calculated live cell density from the experimental data (symbols) and fitted exponential decay (line). Adapted with modifications from Radisic et al. 2006c.

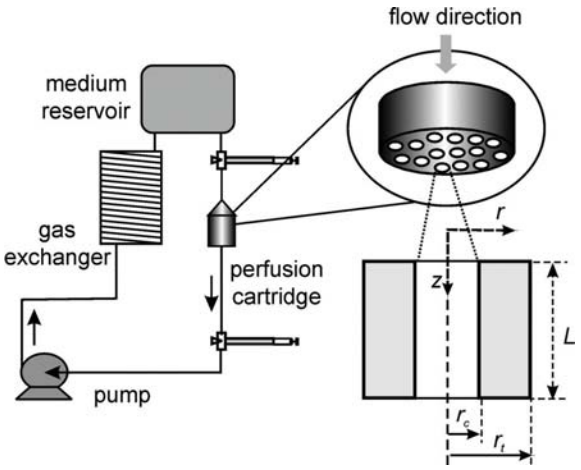

Figure 5: Biomimetic cardiac culture system. Cardiac cells were seeded onto channeled scaffolds and each cell-polymer construct was fitted into a perfusion cartridge connected to a perfusion loop incorporating a medium reservoir and a gas exchanger. Two syringes served for medium exchange and extraction of gas bubbles. Unidirectional medium flow at a physiologic velocity was provided by a multichannel peristaltic pump. For mathematical modeling purposes, the construct is envisioned as an array of cylindrical domains, each representing a channel allowing medium flow and surrounded with a tissue space.

tissue. Each cartridge was connected to a perfusion loop with the total volume of 30 ml, which incorporated a reservoir bag and a gas exchanger (a coil of silicone tubing, 3 m long). Constructs were subjected to unidirectional medium flow by a multichannel peristaltic pump (Fig. 5) at a flow rate of 0.1 ml/min corresponding to the velocity of 560 μm/s (comparable to that of blood flow in native heart).

Furthermore, to mimic the role of hemoglobin, the culture medium was supplemented with a synthetic oxygen carrier (Oxygent^{TM}). Oxygent^{TM} is a 60%w/v (32%v/v) phospholipid stabilized emulsion of perfluorooctyl bromide as a principal component and a small percentage of perfluorodecyl bromide (Kraft et al., 1998). Since perfluorocarbon (PFC) droplets are immiscible with the aqueous phase, they served as rechargeable oxygen reservoirs, replenishing oxygen in the aqueous phase of culture medium by diffusion. Overall, the oxygen partial pressures measured in the aqueous phase of PFC-supplemented and unsupplemented (control) medium were the same, and the PFC particles replenished oxygen consumed by the cells without increasing oxygen concentration in the aqueous phase of culture medium.

3.3 Cardiac tissue engineering in the biomimetic culture system

The concentration of PFC emulsion in the circulating medium of $\sim$ 5.4 %v/v induced significantly lower oxygen decrease in medium passing through the tissue construct (28 mmHg) as compared to the constructs perfused with control culture medium (45 mmHg) (Radisic et al., 2006a). Higher availability of oxygen resulted in markedly and significantly higher contents of DNA and cardiac proteins (troponin I and connexin-43), as well as in enhanced contractile properties of tissue constructs cultured with the PFC supplemented medium as compared to those cultured in control medium (Fig. 6) (Radisic et al., 2006a).

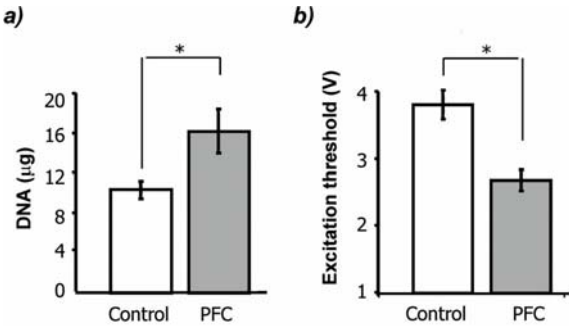

Figure 6: Effects of medium supplementation with PFC emulsion on properties of cardiac tissue constructs continuously perfused for 3 days. a) DNA contents in constructs cultivated in the control and PFC supplemented medium. *Significant difference between the groups by rank-sum test ($p<0.05$), ave. $\pm$SE ($n = 4$). b) Contractile properties of constructs cultivated in the control and PFC supplemented medium: excitation thresholds (V), measured as the minimal amplitude of electrical stimuli (square pulses, 2 ms duration, 60 bpm) needed to induce synchronous macroscopic contractions of the constructs. *Significant difference between the groups by t-test ($p<0.05$), ave. $\pm$SE ($n = 4$-7). Adapted with modifications from Radisic et al., 2006.

The enhanced structural and contractile properties of constructs cultured in PFC supplemented medium are indicative of improved development toward an adult cardiac phenotype, which could be correlated to the efficient oxygen supply to the cells, by a combined use of channeled scaffolds and PFC emulsion.

3.4 Mathematical model

In order to predict oxygen concentration profiles within perfused engineered cardiac constructs, a steady-state mathematical model based on the standard Krogh cylinder model was developed (Radisic et al., 2005). The construct was divided into an array of cylindrical domains, each representing a channel surrounded with a tissue space (Fig. 5). The radial component of the velocity vector was assumed to be negligible in the channel lumen. Due to the low hydraulic permeability of the tissue space, no convective transport in the tissue region was assumed. Oxygen transfer in the channel lumen at the steady state is thus carried by convection in axial direction and axial and radial diffusion in the control medium:

$$D_m\left[\frac{1}{r}\frac{\partial}{\partial r}\left(r\frac{\partial C_m}{\partial r}\right)+\frac{\partial^2 C_m}{\partial z^2}\right]-w\frac{\partial C_m}{\partial z}=0 \quad (7)$$

where D_m is the oxygen diffusion coefficient in the culture medium, w is the axial medium velocity through the channel and a function of the radial position, and C_m is the oxygen concentration in the culture medium.

In the PFC supplemented medium, oxygen release from PFC droplets has to be included as an additional step. PFC droplets were assumed to be small with uniform oxygen concentration (C_p) near the equilibrium with the oxygen concentration in the aqueous phase (C_a) such that the total oxygen concentration in the emulsion, C_{tot}, is:

$$C_{tot}=(1-\phi)C_a+\phi C_p \quad (8)$$

where ϕ is the fraction of PFC droplets. If the partition coefficient is defined as $K=C_p/C_a$, the eq. (8) can be expressed as:

$$C_{tot}=[1+(K-1)\phi]C_a \quad (9)$$

The governing equation for oxygen transfer in the channel lumen of the constructs perfused with

PFC supplemented medium is then:

$$D_{eff}\left[\frac{1}{r}\frac{\partial}{\partial r}\left(r\frac{\partial C_a}{\partial r}\right)+\frac{\partial^2 C_a}{\partial z^2}\right] - w[1+(K-1)\phi]\frac{\partial C_a}{\partial z}=0 \quad (10)$$

where D_{eff} is the effective diffusion coefficient of oxygen in the culture medium supplemented with PFC.

In the tissue region, both axial and radial diffusion were taken into account while the oxygen consumption rate was assumed to follow Michaelis-Menten kinetics:

$$D_t\left[\frac{1}{r}\frac{\partial}{\partial r}\left(r\frac{\partial C_t}{\partial r}\right)+\frac{\partial^2 C_t}{\partial z^2}\right]-\frac{Q_{\max}C_t}{C_t+C_m}=0 \quad (11)$$

where D_t is the oxygen diffusion coefficient in the tissue space, C_t is the local oxygen concentration in the tissue space, Q_{max} is the maximum oxygen consumption rate, and C_m is the C_t at the half-maximal consumption rate.

For boundary conditions, the inlet and outlet oxygen concentrations in the channel and the tissue regions were set equal to those measured experimentally (C_{in} and C_{out}, respectively). Symmetry conditions were applied at the channel axis ($r = 0$) and at the half distance between two channel centers ($r = r_t$). Finally, at the channel-tissue interface ($r = r_c$) oxygen concentrations in the aqueous phase and the tissue have to be equal and the oxygen diffusion flux across the interface has to be constant. Boundary conditions are summarized in the Table 2.

Table 2: Boundary conditions for the porous tissue construct of the length L, channel radius r_c, and half distance between centers of two channels r_t.

	Channel	**Tissue annulus**
$z = 0$	$0 \le r < r_c$ $C_a = C_{in}$	$0 \le r < r_t$ $C_t = C_{in}$
$z = L$	$0 \le r < r_c$ $C_a = C_{out}$	$0 \le r < r_t$ $C_t = C_{out}$
$0 \le z \le L$	$r = 0$ $\partial C_L/\partial r = 0$	$r = r_t$ $\partial C_t/\partial r = 0$
$0 \le z \le L$ $r = r_c$	$D_a\frac{\partial C_a}{\partial r} = D_t\frac{\partial C_t}{\partial r}$	$C_a = C_t$

Model parameters were determined according to the experimental conditions. The construct geometry was set to the measured values (L = 2 mm, r_c = 165 μm, r_t = 185 μm) as well as the average medium velocity in channels (490 μm/s) and cell density (0.27×10^8 cell/ml). The volume fraction of circulating PFC emulsion droplets (ϕ) was 6.4% volume, which was higher than the nominal fraction due to some settling in the lower portions of the loop. Inlet and outlet oxygen concentrations were measured as C_{in} = 222.5 μM and C_{out} = 152.6 μM in the control medium and C_{in} = 213.0 μM and C_{out} = 177.0 μM in the PFC supplemented medium. Maximum oxygen consumption rate, Q_{max}, was calculated based on the total protein content in constructs cultivated with and without PFC and the maximum oxygen consumption rate of 26.7 nmol/min/mg protein as reported in (Yamada et al., 1985). Total protein content of the constructs cultivated without PFC was 0.624 mg and those cultivated with PFC was 0.743mg. For model predictions, Q_{max}, was determined to be 3.3×10^{-16} mole/cell.s assuming 7.2×10^{-7} mg protein/cell. The parameter C_m was 6.875 μM (Casey and Arthur, 2000). Oxygen diffusion coefficients in the aqueous and tissue phases were set to the values reported in the literature as $D_a = 2.4 \times 10^{-5}$ cm^2/s (Geankoplis, 1993) and $D_t = 2.0 \times 10^{-5}$ cm^2/s (Carrier et al., 2002), respectively. Effective diffusion coefficient of oxygen in the culture medium supplemented with 6.4 % vol. PFC was calculated as $D_{eff} = 2.83 \times 10^{-5}$ cm^2/s (Radisic et al., 2005). Partitioning coefficient K was determined as 20.3 (Radisic et al., 2005). The model was solved using the finite element method and the commercial software FEMLAB 2.2 (Radisic et al., 2005).

Supplementation of the culture medium by PFC emulsion was predicted to improve mass transport by increasing convective term and effective diffusivity of culture medium resulting in increased total oxygen concentration (Fig. 7). PFC particles

served as oxygen reservoirs replenishing it as it was depleted from the aqueous phase in the channel lumen by consumption in the tissue space. The presence of PFC emulsion increased both the axial transport by increasing the apparent convective term (by $(K-1)\phi$), and the radial transport by increasing the effective diffusivity. However, the increase in axial transport contributed $\sim 98\%$ to the increase in oxygen concentration in the tissue space (Radisic et al., 2005).

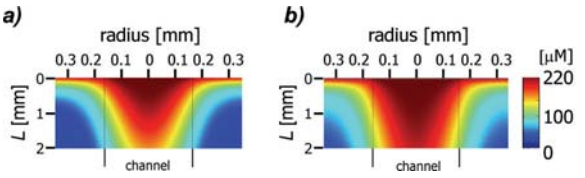

Figure 7: Predictions of oxygen profiles (μM) in a channel and tissue space of a construct with cell density of 0.27×10^8 cell/ml, 330 μm channel diameter and 370 μm wall-to-wall spacing, perfused at a velocity of 490 μm/s with a) control medium, b) medium supplemented with 6.4% volume PFC emulsion; vertical lines designate the channel walls. Adapted with modifications from Radisic et al., 2005.

Model predictions were consistent with experimental findings of higher oxygen concentrations measured at cartridge outlets perfused with PFC-supplemented medium as compared to those perfused with control medium (Radisic et al., 2006a).

However, predictions of oxygen distribution indicate that even at a lower cell density than the physiological (0.27×10^8 vs. 1×10^8 cell/ml) and continuous perfusion of the culture medium supplemented with PFC emulsion, at applied construct geometry, oxygen concentrations in the tissue are maintained above 100 μM only in the construct surface layer and a 50 μm thick zone around each channel (Fig. 7b). These results indicate that the construct geometry and/or cultivation parameters should be changed in order to achieve efficient oxygen supply throughout the tissue volume. Therefore, the mathematical model was applied to predict oxygen distributions in constructs with physiologic cell density (1×10^8 cell/ml) perforated with narrower and more densely packed channels (100 μm in diameter positioned at 100 μm distances). Medium velocity through the channels was set to the experimental value (490 μm/s) comparable to blood velocity found *in vivo* ($\sim$500 μm/s). The medium was assumed to be fully saturated with atmospheric oxygen at the channel inlet (C_{in} = 222.47 μM) while the oxygen concentration was assumed to vary only within the construct i.e. at the construct outlet oxygen concentration stops varying as a function of bioreactor length:

$$\frac{\partial C_a(r,L)}{\partial z} = 0 \tag{12}$$

It was also assumed that the culture medium at the outlet was well mixed, with no variations in the radial direction so that the mean value in the aqueous phase at the construct outlet was set as the outlet oxygen concentration for the tissue space as:

$$C_t(r,L) = \frac{\int_0^{r_c} C_a(r,L) w r dr}{\int_0^{r_c} w r dr} \tag{13}$$

Model predictions indicated that continuous perfusion with medium supplemented with 6.4 % vol. PFC induced significant increase in predicted oxygen distribution in the tissue as compared to the control medium (Fig. 8a). However, even at such conditions, the lower half of the construct still remained poorly supplied with oxygen (Fig. 8a). Only when medium velocity was increased to the value of 1.35 mm/s, efficient oxygen supply throughout the tissue space was predicted, provided that the medium was supplemented with PFC emulsion (Fig. 8b).

The results of mathematical modeling distinctly indicate the importance of the biomimetic approach in cardiac tissue engineering, with oxygen supply being crucial for survival of cardiomyocytes. Clearly, *in vivo* myocardial environment with network of capillaries, $\sim$7 μm in diameter, spaced at approximate distances of 30 μm, and continually supplied with blood containing hemoglobin as an oxygen carrier are an utmost

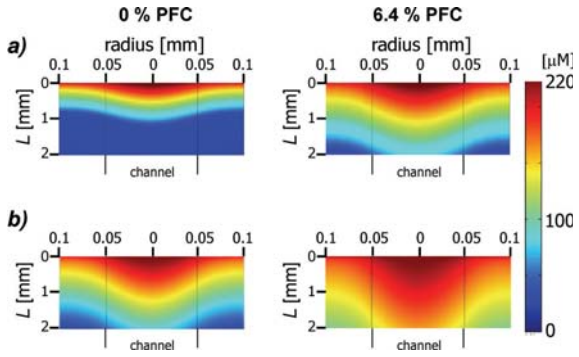

Figure 8: Predictions of oxygen profiles (μM) in a channel and tissue space of a construct with cell density of 1×10^8 cell/ml, 100 μm channel diameter and 100 μm wall-to-wall spacing, perfused at a velocity of: a) 490 μm/s and b) 1.35 mm/s with control medium (0 % PFC, left panels) and medium supplemented with 6.4% volume PFC emulsion (right panels); vertical lines designate channel walls. Adapted with modifications from Radisic et al., 2005.

goal of tissue engineering system design. Channeled scaffolds, with the aim to produce very narrow and densely packed channels, medium supplementation with synthetic oxygen carriers and continuous construct perfusion at physiologic velocities are currently being employed as a feasible attempt towards an ideal biomimetic system.

4 Conclusions

Efficient mass transport is one of the key requirements in the design of tissue engineering systems in order to provide adequate delivery of nutrients, oxygen and regulatory molecules to the cells and remove CO_2 and metabolites. Delivery of oxygen is often critical in order to support cell viability throughout the tissue structure. Tissue engineering systems should rely on the integrated design of the bioreactor configuration and cell support template aimed at adjusting mass transfer rates to the particular cell and tissue type. In this paper, we have reviewed approaches to design and mathematical modeling of tissue engineering systems for cultivation of cartilage and myocardium, which significantly differ in respect to their demands for oxygen supply.

Relatively low oxygen requirements of cartilage were shown to be met using rotating bioreactors that (1) control the level of oxygen in culture medium (via gas exchange with incubator air), (2) eliminate external gradients via convective transport around the tissue surfaces and (3) allow diffusional transport between the construct surfaces and inner tissue phase. Mathematical modeling has confirmed the results of numerous *in vitro* as well *in vivo* studies showing that chondrocytes are well adapted to hypoxic conditions. Efficient oxygen supply was predicted to have a rather activating effect on cells seeded on 3D scaffolds for GAG synthesis in the early phase of construct cultivation. In later cultivation stages, despite the predicted oxygen concentrations as low as $\sim$10 μM in the construct center, some other, possibly self-secreted factors enhanced uniform tissue regeneration.

In contrast, cardiac cells were shown to be much more sensitive to oxygen deficiency and to exhibit much higher oxygen utilization rate as compared to chondrocytes. Although physiological cell densities in the two tissues are similar ($\sim 1 \times 10^8$ cell/ml), maximal oxygen consumption rate for cardiomyocytes was reported to be 2 orders of magnitude higher than the value reported for chondrocytes (3.3×10^{-16} vs. 1.86×10^{-18} mole/cell.s, respectively). In addition, *in vitro* studies have shown that cardiomyocytes can not survive at oxygen concentrations below $\sim$100 μM as opposed to chondrocytes, which were shown *in vitro* and *in vivo* to be metabolically active at oxygen concentrations down to $\sim 10\mu$M. Due to these differences, tissue engineering systems commonly used for cultivation of cartilaginous tissues have shown to be inappropriate for cardiac tissue engineering, which demanded a biomimetic approach. In specific, highly porous channeled scaffolds mimicking a capillary network, medium supplemented with oxygen carriers fulfilled the role of hemoglobin in blood, and tissue perfusion at physiologic velocities was used to enhance oxygen delivery, resulting in an improved structural and contractile properties of engineered cardiac constructs. Mathematical

modeling of both tissue engineering systems was shown to support experimental findings and provide insight into the effects and mechanisms of oxygen transfer *in vitro.* Thus mathematical modeling was an indispensable tool for understanding and optimizing the cultivation of functional equivalents of native tissues for potential clinical applications.

Acknowledgement: The work described in this article was funded by the Ministry of Science and Environmental Protection of the Republic of Serbia, grant 142075 (BO), NIH grants P41 EB002520-01, R01 DE016525 and R01 HL076485-01 (GV), ARTEC and NSERC Discovery Grant (MR).

References

Brighton, C.T.; Heppenstall, R.B. (1971): Oxygen tension in zones of the epiphyseal plate, the metaphysis and diaphysis. *J. Bone Joint Surg. Am*., vol. 53A, pp. 719-728.

Brilla, C.G.; Maisch, B.; Rupp, H.; Sunck, R.; Zhou, G.; Weber, K.T. (1995): Pharmacological modulation of cardiac fibroblast function. *Herz,* vol. 20, pp. 127-135.

Buckwalter, J.A.; Mankin, H.J. (1997): Articular cartilage, part I: Tissue design and chondrocyte-matrix interactions. *J. Bone Joint Surg. Am*., vol. 79A, pp. 600-611.

Bursac, N.; Papadaki, M.; Cohen, R.J.; Schoen, F.J.; Eisenberg, S.R.; Carrier, R.; Vunjak-Novakovic, G.; Freed, L.E. (1999): Cardiac muscle tissue engineering: toward an in vitro model for electrophysiological studies. *Am. J. Physiol. Heart Circ. Physiol*., vol. 277, pp. H433-H444.

Carrier, R.L.; Rupnick, M.; Langer, R.; Schoen, FJ; Freed, L.E.; Vunjak-Novakovic, G. (2002): Perfusion improves tissue architecture of engineered cardiac muscle. *Tissue Eng.,* vol. 8, pp. 175–188.

Casey, T.M.; Arthur, P.G. (2000): Hibernation in noncontracting mammalian cardiomyocytes. *Circulation,* vol. 102, pp. 3124–3129.

Fournier, R.L. (1998): *Basic Transport Phenomena in Biomedical Engineering*. Taylor & Francis, Philadelphia.

Freed, L.E.; Vunjak-Novakovic, G. (1995): Cultivation of cell-polymer constructs in simulated microgravity. *Biotechnol. Bioeng*., vol. 46, pp. 306-313.

Freed, L.E.; Hollander, A.P.; Martin, I.; Barry, J.R.; Langer, R.; Vunjak-Novakovic, G. (1998): Chondrogenesis in a cell-polymer-bioreactor system. *Exp. Cell Res.,* vol. 240, pp. 58-65.

Geankoplis, C.J. (1993): *Transport Processed and Unit Operations* (3rd ed.). Prentice-Hall, Englewood Cliffs, NJ.

Hascall, V.C.; Sandy, J.D.; Handley, C.J. (1999): Regulation of proteoglycan metabolism in articular cartilage. In: Archer, C.W. (ed.): *Biology of the synovial joint*. Harwood Academic Publishers, Chapter 7.

Haselgrove, J.C.; Shapiro, I.M.; Silverton, S.F. (1993): Computer Modeling of the Oxygen Supply and Demand of Cells of the Avian Growth Cartilage, *Am. J. Physiol*., vol. 265 (*Cell Physiol*., vol. 34) C497-C506.

Hogea, C.S.; Murray B.T.; Sethian J.A. (2005): Implementation of the level set method for continuum mechanics based tumor growth models, *FDMP: Fluid Dynamics and Materials Processing*, vol. 1: pp. 109-130.

Hogea, C.S.; Murray B.T.; Sethian J.A. (2006): Simulating complex tumor dynamics from avascular to vascular growth using a general level-set method, *J. Math. Biol*., vol. 53, pp. 86-134.

Kraft, M.P.; Riess, J.G.; Weers, J.G. (1998): The design and engineering of oxygen-delivering fluorocarbon emulsions. In: S. Benita (ed) *Submicron Emulsions in Drug Targeting and Delivery*, Harwood Academic Publishers, Amsterdam, pp. 235-333.

Lappa M. (2003): Organic tissues in rotating bioreactors: fluid-mechanical aspects, dynamic growth model, and morphological evolution, *Biotechnol. Bioeng*., vol. 84, pp. 518-532.

Lappa, M. (2005): A CFD level-set method for soft tissue growth: theory and fundamental equations, *J. Biomechanics*, vol. 38, pp. 185-190.

MacKenna, D.A.; Omens, J.H.; McCulloch, A.D.; Covell, J.W. (1994): Contribution of collagen matrix to passive left ventricular mechanics in isolated rat heart. *Am. J. Physiology,* vol. 266, pp. H1007-H1018.

Malda, J.; Rouwkema, J.; Martens, D.E.; Le Comte, E.P.; Kooy, F.K.; Tramper, J.; van Blitterswijk, C.A.; Riesle, J. (2004) Oxygen gradients in tissue-engineered PEGT/PBT cartilaginous constructs: Measurement and modeling. *Biotechnol. Bioeng.,* vol. 86, pp. 9-18.

Martin, I.; Obradovic, B.; Freed, L.E.; Vunjak-Novakovic, G. (1999): A method for quantitative analysis of glycosaminoglycan distribution in cultured natural and engineered cartilage. *Ann. Biomed. Eng*., vol. 27, pp. 656-662.

Martin, I.; Wendt, D.; Heberer, M. (2004): The role of bioreactors in tissue engineering. *Trends Biotechnol*., vol. 22, pp. 80-86.

Muschler, G.F.; Nakamoto, C.; Griffith, L.G. (2004): Engineering principles of clinical cell-based tissue engineering. *J. Bone Joint Surg. Am*., vol. 86-A, pp. 1541-1558.

Obradovic, B.; Freed, L.E.; Langer, R.; Vunjak-Novakovic, G. (1997): Bioreactor studies of natural and engineered cartilage metabolism. In: N.A. Peppas, D.J. Mooney, A.G. Mikos and L. Brannon-Peppas, (eds.) *Proceedings of the Topical Conference on Biomaterials, Carriers for Drug Delivery, and Scaffolds for Tissue Engineering*, pp. 335-337. AIChE, New York.

Obradovic, B.; Carrier, R.L.; Vunjak-Novakovic, G.; Freed, L.E. (1999): Gas exchange is essential for bioreactor cultivation of tissue engineered cartilage. *Biotechnol. Bioeng*., vol. 63, pp. 197-205.

Obradovic, B.; Meldon, J.H.; Freed, L.E.; Vunjak-Novakovic, G. (2000): Glycosaminoglycan deposition in engineered cartilage: Experiments and mathematical model. *AIChE J*., vol. 46, pp. 1860-1871.

O'Hara, B.P.; Urban, J.P.G.; Maroudas, A. (1990): Influence of cyclic loading on the nutrition of articular cartilage. *Ann. Rheum. Dis*., vol. 49, pp. 536-539.

Radisic, M.; Euloth, M.; Yang, L.; Langer, R.; Freed, L.E.; Vunjak-Novakovic, G. (2003): High density seeding of myocyte cells for tissue engineering. *Biotechnol Bioeng.,* vol. 82, pp. 403–414.

Radisic, M.; Deen, W.; Langer, R.; Vunjak-Novakovic, G. (2005): Mathematical model of oxygen distribution in engineered cardiac tissue with parallel channel array perfused with culture medium containing oxygen carriers. *Am. J. Physiol. Heart Circ. Physiol.*, vol. 288, pp. H1278-H1289.

Radisic, M.; Park, H.; Chen, F.; Salazar-Lazzaro, J.E.; Wang, Y.; Dennis, R.G.; Langer, R.; Freed, L.E.; Vunjak-Novakovic, G. (2006a): Biomimetic approach to cardiac tissue engineering: Oxygen carriers and channeled scaffolds. *Tissue Eng*., vol. 12, pp. 1-15.

Radisic, M.; Cannizzaro, C.; Vunjak-Novakovic, G. (2006b): Scaffolds and fluid flow in cardiac tissue engineering, *FDMP: Fluid Dynamics and Materials Processing*, vol. 2, pp. 1-15.

Radisic, M.; Malda, J.; Epping, E.; Geng, W.; Langer, R.; Vunjak-Novakovic, G. (2006c): Oxygen gradients correlate with cell density and cell viability in engineered cardiac tissue. *Biotechnol. Bioeng*., vol. 93, pp. 332-343.

Randers-Eichorn, L.; Bartlett, R.; Frey, D.; Rao, G. (1996): Noninvasive oxygen measurements and mass transfer considerations in tissue culture flasks. *Biotechnol. Bioeng*., vol. 51, pp. 466-478.

Urban, J.P.G. (1994): The chondrocyte: a cell under pressure. *Br. J. Rheumatol*., vol. 33, pp. 901-908.

Vunjak-Novakovic, G.; Obradovic, B.; Martin, I.; Bursac P; Langer, R.; Freed, L.E. (1998): Dynamic cell seeding of polymer scaffolds for cartilage tissue engineering. *Biotechnol Prog*. vol. 14, pp. 193-202.

Vunjak-Novakovic, G.; Martin, I.; Obradovic, B.; Treppo, S.; Grodzinsky, A.J.; Langer, R.; Freed, L.E. (1999): Bioreactor cultivation conditions modulate the composition and mechanical properties of tissue engineered cartilage. *J. Or-*

thop. Res., vol. 17, pp. 130-138.

Wang, Y.; Ameer, G.A.; Sheppard, B.J.; Langer, R. (2002): A tough biodegradable elastomer. *Nat. Biotechnol*., vol. 20, pp. 602-606.

Yamada, T.; Yang, J.J.; Ricchiuti, N.V.; Seraydarian, M.W. (1985): Oxygen consumption of mammalian myocardial-cells in culture—measurements in beating cells attached to the substrate of the culture dish. *Anal. Biochem.,* vol. 145, pp. 302–307.